5-Alkyl-2-(alkylthio)-6-(2,6-dihalophenylmethyl)-3,4-dihydropyrimidin-4(3*H*)-ones: Novel Potent and Selective Dihydro-alkoxy-benzyl-oxopyrimidine Derivatives

Antonello Mai,[§] Marino Artico,*[,§] Gianluca Sbardella,[§] Silvio Massa,[†] Ettore Novellino,[‡] Giovanni Greco,[▽] Anna Giulia Loi,[||] Enzo Tramontano,[||] Maria Elena Marongiu,[||] and Paolo La Colla*[,||]

Dipartimento di Studi Farmaceutici, Istituto Pasteur-Fondazione Cenci Bolognetti, Università degli Studi di Roma "La Sapienza", P.le A. Moro 5, I-00185 Roma, Italy, Dipartimento Farmaco Chimico Tecnologico, Università degli Studi di Siena, Banchi di Sotto 55, I-53100 Siena, Italy, Dipartimento di Scienze Farmaceutiche, Università degli Studi di Salerno, P.za Vittorio Emanuele 9, I-84084 Penta (Salerno), Italy, Dipartimento di Chimica Farmaceutica e Tossicologica, Università degli Studi di Napoli "Federico II", via D. Montesano 49, I-80731 Napoli, Italy, and Dipartimento di Biologia Sperimentale, Sezione di Microbiologia, Università degli Studi di Cagliari, V.le Regina Margherita 45, I-09124 Cagliari, Italy

Received April 30, 1998

Molecular modeling analysis of compounds belonging to the recently published series of dihydro-alkoxy-benzyl-oxopyrimidines (DABOs), such as S-DABOs and DATNOs, gave support to the design of new 2,6-disubstituted benzyl-DABO derivatives as highly potent and specific inhibitors of the HIV-1 reverse transcriptase (RT). To follow up on the novel DABO derivatives, we decided to investigate the effect of electron-withdrawing substituents in the benzyl unit of the S-DABO skeleton versus their anti-HIV-1 activity. Such chemical modifications impacted the inhibitory activity, especially when two halogen units were introduced at positions 2 and 6 in the phenyl portion of the benzyl group bound to C-6 of the pyrimidine ring. Various 5-alkyl-2-(alkyl(or cycloalkyl)thio)-6-(2,6-dichloro(or 2,6-difluoro)phenylmethyl)-3,4-dihydropyrimidin-4(3*H*)-ones were then synthesized and tested as anti-HIV-1 agents in both cell-based and enzyme (recombinant reverse transcriptase, rRT) assays. Among the various mono- and disubstituted phenyl derivatives, the most potent were those containing a 6-(2,6-difluorophenylmethyl) substituent (F-DABOs), which showed EC_{50}'s ranging between 40 and 90 nM and selectivity indexes up to ≥5000. An excellent correlation was found between EC_{50} and IC_{50} values which confirmed that these compounds act as inhibitors of the HIV-1 RT. The structure−activity relationships of the newly synthesized pyrimidinones are presented herein.

Currently available drugs for AIDS therapy are divided into two groups: those that prevent infection of target cells (nucleoside (NRTIs) and nonnucleoside reverse transcriptase inhibitors (NNRTIs)) and those that prevent HIV-1-infected cells from yielding infectious viruses (protease inhibitors).[1] Monotherapy with antiretroviral agents has shown limited effects, very likely due to the interplay of phenomena such as: (1) high viral loads and multiplication rates of HIV-1, (2) incomplete inhibition of viral replication, and (3) emergence of drug-resistant mutants.[2] For this reason, combination therapies with two or more drugs have been proposed for a more effective treatment of AIDS.[3] Potent suppression of HIV-1 replication over prolonged periods has been accomplished with regimens including reverse transcriptase (RT) and protease inhibitors,[4] although on stopping therapies viremia has rapidly reappeared. In the attempt to obtain better results, research is now focused on exploiting new targets and enhancements of "old" drugs. Among the latter, new NNRTIs possibly endowed with better pharmacokinetic profiles, such as capability to inhibit clinically relevant mutants and, hopefully, to minimize the HIV-1 multiplication,[5] are being pursued.

Chart 1. Dihydro-alkoxy-benzyl-oxopyrimidines (DABOs) and Related Derivatives

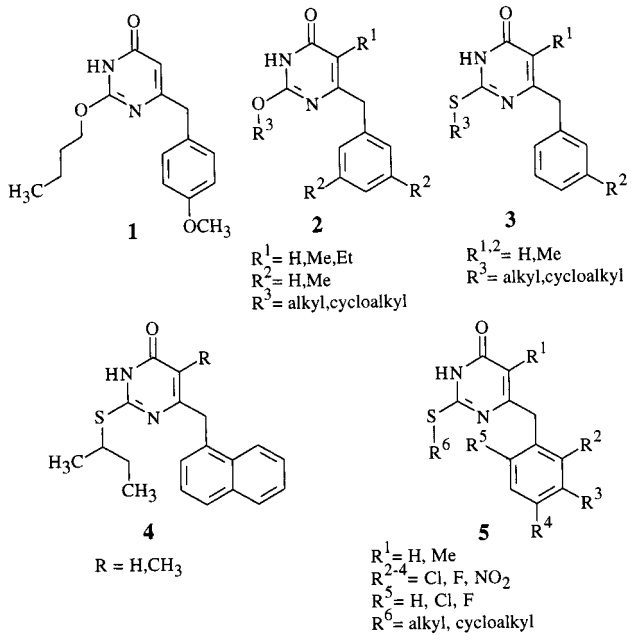

Numerous classes of NNRTIs have been discovered with dihydro-alkyloxy-benzyl-oxopyrimidines (DABOs) being one of them. The lead compound, an isotrimethoprim derivative (**1**, Chart 1), has been synthesized as a possible dihydrofolate reductase inhibitor, and when

* To whom correspondence should be sent.
[§] Università degli Studi di Roma "La Sapienza".
[†] Università degli Studi di Siena.
[‡] Università degli Studi di Salerno.
[▽] Università degli Studi di Napoli "Federico II".
[||] Università degli Studi di Cagliari.

10.1021/jm980260f CCC: $18.00
Published on Web 02/05/1999

tested against HIV-1 because of its structural similarity with HEPT,[6,7] it was a selective, although not very potent, HIV-1 inhibitor.[8]

On the basis of these findings, various oxopyrimidines (**2**, **3**) have been synthesized and found to be specific HIV-1 inhibitors targeted at the reverse transcriptase.[9−12] Structure−activity relationship (SAR) studies have shown that the presence of the C-2 alkoxy (DABO)/alkylthio (S-DABO) side chain is a structural determinant for the antiviral activity of these compounds, whereas the length and type of substituent at C-2 (C_{1-6} alkyl-, isoalkyl-, or cycloalkylthio), the substituent at C-5 (H, Me, or Et), and the presence of a monomethyl (3) or dimethyl (3,5) substitution in the phenyl portion of the benzyl moiety have modulatory effects on potency.[12] However, (1) modifications of the pyrimidine base such as N-3 alkylations, (2) introduction of a variety of substituents at C-4, (3) shift of the benzyl group from C-6 to C-5, (4) decrease or increase of the distance between the pyrimidine and the phenyl ring, and (5) replacement of the C-6 benzyl with smaller (propyl) substituents have led to substantial loss of activity. The only exception has been the replacement of the C-6 benzyl with a bulkier substituent such as 1-naphthylmethyl (DATNOs, **4**).[13]

The possible binding mode of the above S-DABOs and DATNOs to the nonnucleoside binding site (NNBS) of the HIV-1 RT was recently examined in our laboratory through molecular modeling methods based on the crystal structure of the RT/HEPT complex reported by Ren et al.[14] The results of these modeling studies prompted the synthesis and biological evaluation of novel DABOs **5** bearing fluorine or chlorine atoms at the 2- and 6-positions of the phenyl ring. A priori, the 2,6-dihalogenation was expected to improve a putative π-stacking interaction between the electron-deficient benzene ring of the ligand and the electron-rich benzene ring of Tyr188 located in the nonnucleoside binding cleft of RT. To better define the effects of electron-withdrawing substituents on the inhibitory activity, additional DABOs were designed featuring a fluorine, chlorine, or nitro group at various positions of the phenyl ring. In the herein series, the pyrimidine has C-2 alkylthio substituents (e.g., methyl, isopropyl, isobutyl, *n*-butyl, *sec*-butyl, cyclopentyl, and cyclohexyl) and C-5 substituents of hydrogen (uracil) or methyl (thymine).

Chemistry

The ethyl arylacetylacetates, needed for the pyrimidine syntheses, were prepared by several methods. One method involved Claisen condensation of ethyl arylacetates or aroyl chlorides with ethyl acetate[15] or, alternatively, acylation of diethyl malonate followed by partial hydrolysis and decarboxylation[16,17] (classic methods). The second approaches are based on the use of ethylmalonic acid,[18] *tert*-butyl ethyl malonate,[19] or Meldrum's acid and subsequent ethanolysis.[20−22] However, these methods can lead to undesired byproducts or retro-condensation reactions, and they afford the required β-oxoesters in moderate or low yields. To obviate these disadvantages, we prepared the ethyl arylacetylacetates **7** by a simple and high-yielding method by the reaction of potassium monoethyl malonate or methyl malonate with (arylacetyl)imidazolides **6** in the presence

Scheme 1[a]

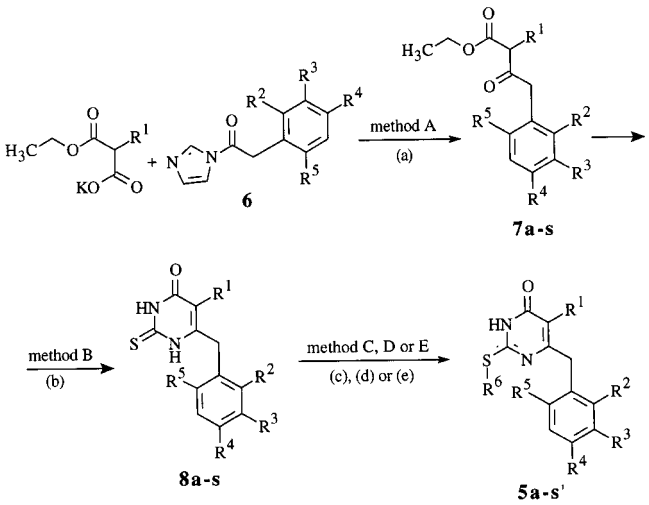

[a] (a) (1) $(C_2H_5)_3N$, $MgCl_2$, CH_3CN, rt then reflux, (2) 13% HCl; (b) (1) C_2H_5ONa, NH_2CSNH_2, C_2H_5OH, reflux, (2) 2 N HCl; (c) CH_3I, DMF, rt; (d) R^6 halide, K_2CO_3, DMF, rt; (e) $C_6H_{11}I$, K_2CO_3, DMF, 80 °C.

Scheme 2[a]

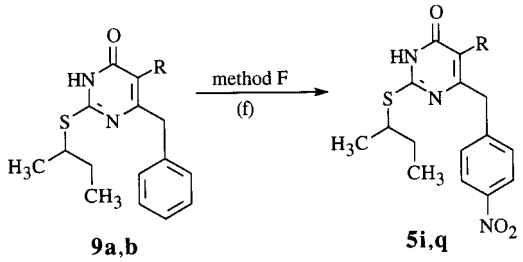

[a] (f) HNO_3, H_2SO_4, 0 °C then rt.

of the magnesium dichloride−triethylamine system. When compared to our previously reported procedure for β-oxoester preparation,[13] this new method afforded almost quantitative yields of ethyl arylacetylacetates **7**, which were sufficiently pure to be used for subsequent reactions without further purification.

Condensation of the above β-oxoesters with thiourea[12,23] afforded the related uracil and thymine derivatives **8**, which were S-alkylated in dry DMF with iodomethane (2 equiv) or with the appropriate haloalkane (or halocycloalkane, 1 equiv) in the presence of potassium carbonate to yield the required 5-alkyl-2-(alkyl(or cycloalkyl)thio)-3,4-dihydro-6-(substituted phenylmethyl)pyrimidine-4(3*H*)-ones **5** (Scheme 1).

2-(*sec*-Butylthio)-3,4-dihydro-6-(4-nitrophenylmethyl)-pyrimidin-4(3*H*)-one derivatives **5i**,**q** were obtained by direct nitration of 2-(*sec*-butylthio)-3,4-dihydro-6-(phenylmethyl)pyrimidin-4(3*H*)-one and its 5-methyl derivative[12] (Scheme 2). Chemical and physical data for derivatives **5**, **7**, and **8** are reported in Tables 1 and 2.

Results and Discussion

Computer-Assisted Design of Novel DABOs. The computational work was carried out by molecular mechanics (Tripos force field[26]), conformational analysis, docking, and graphics routines available within the SYBYL program.[27] Details of these procedures are described in the Experimental Section, whereas the results are summarized below.

Table 1. Physical and Chemical Data of Compound **5**

compd	substituent						mp, °C	recryst solvent[a]	method of synthesis	yield, %	formula[b]
	R^1	R^2	R^3	R^4	R^5	R^6					
5a	H	Cl	H	H	H	*s*-butyl	120−121	a	D	58	$C_{15}H_{17}ClN_2OS$
5b	H	H	Cl	H	H	*s*-butyl	98−99	b	D	92	$C_{15}H_{17}ClN_2OS$
5c	H	H	H	Cl	H	*s*-butyl	125−126	b	D	74	$C_{15}H_{17}ClN_2OS$
5d	H	F	H	H	H	*s*-butyl	106−107	a	D	68	$C_{15}H_{17}FN_2OS$
5e	H	H	F	H	H	*s*-butyl	96−97	b	D	67	$C_{15}H_{17}FN_2OS$
5f	H	H	H	F	H	*s*-butyl	98−99	c	D	94	$C_{15}H_{17}FN_2OS$
5g	H	NO_2	H	H	H	*s*-butyl	148.0−148.5	d	D	68	$C_{15}H_{17}N_3O_3S$
5h	H	H	NO_2	H	H	*s*-butyl	127−128	d	D	54	$C_{15}H_{17}N_3O_3S$
5i	H	H	H	NO_2	H	*s*-butyl	128−130	e	F	100	$C_{15}H_{17}N_3O_3S$
5j	Me	Cl	H	H	H	*s*-butyl	170−171	b	D	68	$C_{16}H_{19}ClN_2OS$
5k	Me	H	Cl	H	H	*s*-butyl	145−146	b	D	75	$C_{16}H_{19}ClN_2OS$
5l	Me	H	H	Cl	H	*s*-butyl	163−165	b	D	79	$C_{16}H_{19}ClN_2OS$
5m	Me	F	H	H	H	*s*-butyl	120.5−121.5	b	D	65	$C_{16}H_{19}FN_2OS$
5n	Me	H	F	H	H	*s*-butyl	146−147	b	D	72	$C_{16}H_{19}FN_2OS$
5o	Me	H	H	F	H	*s*-butyl	154−155	b	D	69	$C_{16}H_{19}FN_2OS$
5p	Me	H	NO_2	H	H	*s*-butyl	163−164	b	D	88	$C_{16}H_{19}N_3O_3S$
5q	Me	H	H	NO_2	H	*s*-butyl	178−180	b	F	100	$C_{16}H_{19}N_3O_3S$
5r	H	Cl	H	H	Cl	*s*-butyl	237−238	f	C	98	$C_{12}H_{10}Cl_2N_2OS$
5s	H	Cl	H	H	Cl	*s*-butyl	230−231	f	D	81	$C_{14}H_{14}Cl_2N_2OS$
5t	H	Cl	H	H	Cl	*s*-butyl	153−154	b	D	62	$C_{15}H_{16}Cl_2N_2OS$
5u	H	Cl	H	H	Cl	*s*-butyl	143.5−144.5	b	D	56	$C_{15}H_{16}Cl_2N_2OS$
5v	H	Cl	H	H	Cl	*s*-butyl	183−184	d	D	55	$C_{15}H_{16}Cl_2N_2OS$
5v	H	Cl	H	H	Cl	*s*-butyl	185−186	b	D	54	$C_{16}H_{16}Cl_2N_2OS$
5x	H	Cl	H	H	Cl	*s*-butyl	200−201	d	E	49	$C_{17}H_{18}Cl_2N_2OS$
5y	H	F	H	H	F	*s*-butyl	197−198	f	C	95	$C_{12}H_{10}F_2N_2OS$
5z	H	F	H	H	F	*s*-butyl	174−175	b	D	74	$C_{14}H_{14}F_2N_2OS$
5a′	H	F	H	H	F	*s*-butyl	126−127	b	D	46	$C_{15}H_{16}F_2N_2OS$
5b′	H	F	H	H	F	*s*-butyl	136−137	b	D	49	$C_{15}H_{16}F_2N_2OS$
5c′	H	F	H	H	F	*s*-butyl	149−150	a	D	48	$C_{15}H_{16}F_2N_2OS$
5d′	H	F	H	H	F	*s*-butyl	168−169	b	D	45	$C_{16}H_{16}F_2N_2OS$
5e′	H	F	H	H	F	*s*-butyl	164−165	f	E	40	$C_{17}H_{18}F_2N_2OS$
5f′	Me	Cl	H	H	Cl	*s*-butyl	260−261	d	C	93	$C_{13}H_{12}Cl_2N_2OS$
5g′	Me	Cl	H	H	Cl	*s*-butyl	241−242	b	D	78	$C_{15}H_{16}Cl_2N_2OS$
5h′	Me	Cl	H	H	Cl	*s*-butyl	179−180	b	D	52	$C_{16}H_{18}Cl_2N_2OS$
5i′	Me	Cl	H	H	Cl	*s*-butyl	208−209	b	D	63	$C_{16}H_{18}Cl_2N_2OS$
5j′	Me	Cl	H	H	Cl	*s*-butyl	204−205	b	D	53	$C_{16}H_{18}Cl_2N_2OS$
5k′	Me	Cl	H	H	Cl	*s*-butyl	252−253	d	D	49	$C_{17}H_{18}Cl_2N_2OS$
5l′	Me	Cl	H	H	Cl	*s*-butyl	237−238	b	E	48	$C_{18}H_{20}Cl_2N_2OS$
5m′	Me	F	H	H	F	*s*-butyl	218.5−219.5	f	C	92	$C_{13}H_{12}F_2N_2OS$
5n′	Me	F	H	H	F	*s*-butyl	164−165	b	D	76	$C_{15}H_{16}F_2N_2OS$
5o′	Me	F	H	H	F	*s*-butyl	178−179	b	D	65	$C_{16}H_{18}F_2N_2OS$
5p′	Me	F	H	H	F	*s*-butyl	161−162	b	D	59	$C_{16}H_{18}F_2N_2OS$
5q′	Me	F	H	H	F	*s*-butyl	128−129	c	D	49	$C_{16}H_{18}F_2N_2OS$
5r′	Me	F	H	H	F	*s*-butyl	192−193	b	D	54	$C_{17}H_{18}F_2N_2OS$
5s′	Me	F	H	H	F	*s*-butyl	191−192	b	E	49	$C_{18}H_{20}F_2N_2OS$

[a] Code: a, *n*-hexane/cyclohexane; b, cyclohexane; c, *n*-hexane; d, benzene/cyclohexane; e, diethyl ether/petroleum ether; f, benzene. [b] All compounds were analyzed for C, H, N, S and, when required, Cl and F; analytical results were within ±0.4% of theoretical values.

Chart 2. Previously Reported S-DABOs[12] Used as References in SAR Studies and Molecular Modeling

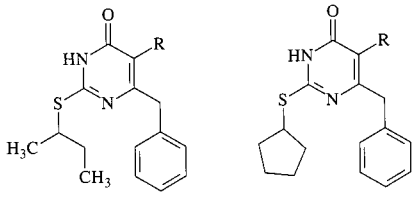

9a R = H
9b R = CH_3

10a R = H
10b R = CH_3

The design of 2,6-dihalogenated DABOs was prompted by inspection of a previously derived model of compound **10b** (Chart 2) docked into the NNBS of HIV-1 RT (unpublished results). Coordinates of the NNBS were taken from the crystal structure of the RT/HEPT complex reported at 3.0 Å resolution by Ren et al.[14] The high degree of similarity between HEPT and DABOs justified the selection of such a complex among those currently available[28] from the Brookhaven Protein Data Bank.[29] The choice of modeling a 2-(cyclopentylthio)-5-methyl derivative, such as **10b**, was based on two considerations: (i) the cyclopentyl group is fairly rigid and lacks chiral centers, and its medium size makes it representative of both small (methyl) and large (*sec*-butyl) groups of the 2-alkylthio side chain; (ii) it was soon realized that any conformation energetically allowed to a 5-methyl derivative could also be attained by the less encumbered 5-desmethyl counterpart.

The model of the RT/**10b** complex, like those later developed for other DABOs of general formula **5**, was derived through the following steps: (i) manual alignment of the 2-(cyclopentylthio)thymine moiety within the NNBS using the enzyme-bound conformation of HEPT as template; (ii) systematic search of the ligand conformation in which the 6-arylmethyl chain fills the largest volume within the binding cleft; (iii) geometry optimization of the resulting complex by keeping the protein backbone atoms fixed.

Figure 1 shows the theoretical binding mode of **5r′** to the NNBS. The following features of the model are worthy to be outlined. The thymine and 2,6-difluorophen-

Table 2. Physical and Chemical Data of Compounds **7** and **8**

	substituent								
compd	R^1	R^2	R^3	R^4	R^5	mp, °C	recryst solvent[a]	yield, %	formula[a]
7a	H	Cl	H	H	H	oil		85	$C_{12}H_{13}ClO_3$[b]
7b	H	H	Cl	H	H	oil		94	$C_{12}H_{13}ClO_3$
7c	H	H	H	Cl	H	oil		90	$C_{12}H_{13}ClO_3$
7d	H	F	H	H	H	oil		85	$C_{12}H_{13}FO_3$
7e	H	H	F	H	H	oil		94	$C_{12}H_{13}FO_3$
7f	H	H	H	F	H	oil		92	$C_{12}H_{13}FO_3$
7g	H	NO_2	H	H	H	56−57	diethyl ether/petroleum ether	98	$C_{12}H_{13}NO_5$[c]
7h	H	H	NO_2	H	H	59−60	benzene/cyclohexane	90	$C_{12}H_{13}NO_5$[d]
7i	Me	Cl	H	H	H	oil		90	$C_{13}H_{15}ClO_3$
7j	Me	H	Cl	H	H	oil		98	$C_{13}H_{15}ClO_3$
7k	Me	H	H	Cl	H	oil		100	$C_{13}H_{15}ClO_3$
7l	Me	F	H	H	H	oil		89	$C_{13}H_{15}FO_3$
7m	Me	H	F	H	H	oil		88	$C_{13}H_{15}FO_3$
7n	Me	H	H	F	H	oil		100	$C_{13}H_{15}FO_3$
7o	Me	H	NO_2	H	H	oil		82	$C_{13}H_{15}NO_5$
7p	H	Cl	H	H	Cl	75−76	*n*-hexane	99	$C_{12}H_{12}Cl_2O_3$
7q	H	F	H	H	F	37−38	*n*-hexane	87	$C_{12}H_{12}F_2O_3$
7r	Me	Cl	H	H	Cl	98−99	*n*-hexane	94	$C_{13}H_{14}Cl_2O_3$
7s	Me	F	H	H	F	oil		87	$C_{13}H_{14}F_2O_3$
8a	H	Cl	H	H	H	240−242	ethanol	43	$C_{11}H_9ClN_2OS$
8b	H	H	Cl	H	H	239−240	ethanol	52	$C_{11}H_9ClN_2OS$
8c	H	H	H	Cl	H	242−243	ethanol	75	$C_{11}H_9ClN_2OS$[e]
8d	H	F	H	H	H	239−241	ethanol	85	$C_{11}H_9FN_2OS$
8e	H	H	F	H	H	220−221	ethanol	60	$C_{11}H_9FN_2OS$
8f	H	H	H	F	H	225−227	ethanol	62	$C_{11}H_9FN_2OS$
8g	H	NO_2	H	H	H	248−249	ethanol	18	$C_{11}H_9N_3O_3S$ [f]
8h	H	H	NO_2	H	H	246−248	ethanol	83	$C_{11}H_9N_3O_3S$
8i	Me	Cl	H	H	H	243−245	ethanol	56	$C_{12}H_{11}ClN_2OS$
8j	Me	H	Cl	H	H	229−230	ethanol	59	$C_{12}H_{11}ClN_2OS$
8k	Me	H	H	Cl	H	262−263 dec	ethanol	64	$C_{12}H_{11}ClN_2OS$
8l	Me	F	H	H	H	246−247	ethanol	52	$C_{12}H_{11}FN_2OS$
8m	Me	H	F	H	H	251−252	ethanol	55	$C_{12}H_{11}FN_2OS$
8n	Me	H	H	F	H	255−256	ethanol	62	$C_{12}H_{11}FN_2OS$
8o	Me	H	NO_2	H	H	268−269	ethanol	46	$C_{12}H_{11}N_3O_3S$
8p	Me	Cl	H	H	Cl	>280	ethanol	78	$C_{11}H_8Cl_2N_2OS$
8q	H	F	H	H	F	>280	ethanol	84	$C_{11}H_8F_2N_2OS$
8r	Me	Cl	H	H	Cl	258−260	ethanol	40	$C_{12}H_{10}Cl_2N_2OS$
8s	Me	F	H	H	F	278−280 dec	ethanol	56	$C_{12}H_{10}F_2N_2OS$

[a] All compounds were analyzed for C, H, N, S and, when required, Cl and F; analytical results were within ±0.4% of theoretical values. [b] Reference 24. [c] Reference 20. [d] Reference 21. [e] Reference 19. [f] Reference 25.

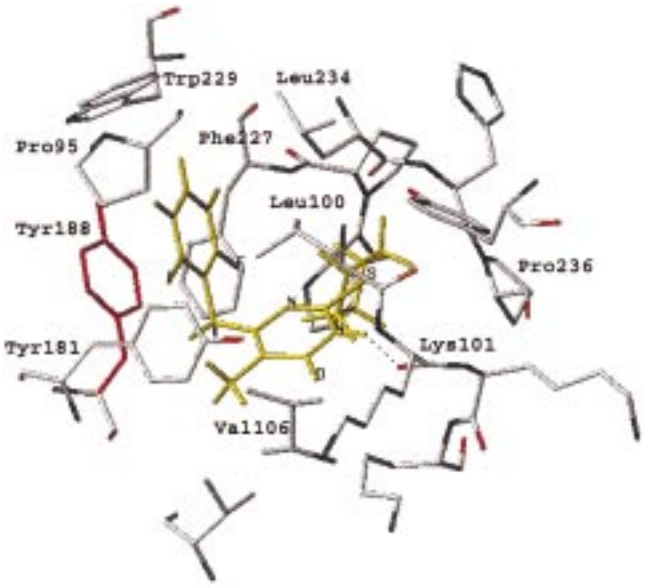

Figure 1. 2,6-Difluoro-DABO (**5r′**) (yellow) docked into the nonnucleoside binding site of RT (only 17 residues are displayed). The Tyr188 side chain, hypothesized to give rise to a favorable π-stacking interaction with the 2,6-difluorophenyl moiety of the ligand, is red.

yl parts of the ligand exhibit a "propeller-like" disposition which is intermediate between the "skewed" and the "butterfly" orientation of the planar rings of HEPT and nevirapine, respectively, in their enzyme-bound conformations.[14,30] The thymine moieties of **5r′** and HEPT occupy the same position in the NNBS, the only difference being a rotation by ca. 30° about one another within the same plane. A hydrogen bond is donated by the 3-NH function of **5r′** to the carbonyl oxygen of Lys101 (N···O distance 3.4 Å) which is analogous to that observed for the RT/HEPT complex (N···O distance 3.1 Å). The 2-cyclopentylthio group fits into a pocket reported to exhibit great flexibility about the Pro236 hairpin[31] which is also occupied by the 1-(2-hydroxyethoxy)methyl substituent of HEPT. The 2,6-difluorobenzyl moiety is surrounded by the side chains of Pro95, Tyr181, Tyr188, Phe227, Trp229, Leu100, and Leu234. Particularly, the electron-rich benzene ring of Tyr188 appears to be optimally oriented for a favorable π-stacking interaction with that of the ligand (made electron-deficient by the two fluorines): the planes of the two aromatic rings are fairly parallel and separated by a distance of 3.8 Å.

Given the many approximations implicit in our docking calculations and the known limitations of molecular mechanics in describing polarization effects and charge-transfer interactions, the 2,6-difluoro- and 2,6-dichloro-DABOs were predicted to be more potent than their corresponding parent compounds on qualitative bases.

Table 3. Cytotoxicity and Anti-HIV-1 Activity of Compound **5**[a]

	substituent									
compd	R^1	R^2	R^3	R^4	R^5	R^6	CC_{50}, μM[b]	EC_{50}, μM[c]	IC_{50}, μM[d]	SI[e]
5a	H	Cl	H	H	H	*s*-butyl	200	1.0	1.6	200
5b	H	H	Cl	H	H	*s*-butyl	116	2.0	1.9	58
5c	H	H	H	Cl	H	*s*-butyl	120	5.0	4.8	24
5d	H	F	H	H	H	*s*-butyl	200	0.26	0.3	769
5e	H	H	F	H	H	*s*-butyl	>200 [f]	0.7	0.6	>286
5f	H	H	H	F	H	*s*-butyl	≥200	8.7	7.4	23
5g	H	NO_2	H	H	H	*s*-butyl	>200	0.25	0.3	>800
5h	H	H	NO_2	H	H	*s*-butyl	157	0.4	0.3	392
5i	H	H	H	NO_2	H	*s*-butyl	151	1.5	1.2	101
5j	Me	Cl	H	H	H	*s*-butyl	>200	0.27	0.4	>741
5k	Me	H	Cl	H	H	*s*-butyl	>200	0.96	0.9	>208
5l	Me	H	H	Cl	H	*s*-butyl	>200	9.5	8.5	>20
5m	Me	F	H	H	H	*s*-butyl	140	0.41	0.4	341
5n	Me	H	F	H	H	*s*-butyl	>200	1.2	1.5	>166
5o	Me	H	H	F	H	*s*-butyl	105	11	13	9.5
5p	Me	H	NO_2	H	H	*s*-butyl	>200	0.35	0.4	>571
5q	Me	H	H	NO_2	H	*s*-butyl	>200	2	1.8	>100
5r	H	Cl	H	H	Cl	Me	>200	3.2	3.0	>62
5s	H	Cl	H	H	Cl	*i*-propyl	>200	1.9	1.5	>105
5t	H	Cl	H	H	Cl	*n*-butyl	>200	0.44	0.5	>454
5u	H	Cl	H	H	Cl	*i*-butyl	>200	0.45	0.6	>444
5v	H	Cl	H	H	Cl	*s*-butyl	>200	0.14	0.1	>1428
5v	H	Cl	H	H	Cl	*c*-pentyl	>200	0.4	0.4	>500
5x	H	Cl	H	H	Cl	*c*-hexyl	>200	0.6	0.4	>333
5y	H	F	H	H	F	Me	≥200	0.81	0.8	≥247
5z	H	F	H	H	F	*i*-propyl	≥200	0.05	0.05	≥4000
5a′	H	F	H	H	F	*n*-butyl	162	0.18	0.20	900
5b′	H	F	H	H	F	*i*-butyl	182	0.14	0.20	1300
5c′	H	F	H	H	F	*s*-butyl	≥200	0.04	0.05	≥5000
5d′	H	F	H	H	F	*c*-pentyl	>200	0.08	0.08	>2500
5e′	H	F	H	H	F	*c*-hexyl	>200	0.08	0.09	>2500
5f′	Me	Cl	H	H	Cl	Me	>200	38	ND[g]	5.2
5g′	Me	Cl	H	H	Cl	*i*-propyl	>200	1.3	1.15	>154
5h′	Me	Cl	H	H	Cl	*n*-butyl	>200	1.1	1.15	>171
5i′	Me	Cl	H	H	Cl	*i*-butyl	>200	1.2	1.10	>166
5j′	Me	Cl	H	H	Cl	*s*-butyl	>200	0.05	0.06	>4000
5k′	Me	Cl	H	H	Cl	*c*-pentyl	>200	1.8	1.7	>111
5l′	Me	Cl	H	H	Cl	*c*-hexyl	>200	22	4.9	>9
5m′	Me	F	H	H	F	Me	200	0.19	0.2	1053
5n′	Me	F	H	H	F	*i*-propyl	>200	0.05	0.05	>4000
5o′	Me	F	H	H	F	*n*-butyl	>200	0.08	0.09	>2500
5p′	Me	F	H	H	F	*i*-butyl	164	0.1	0.09	1640
5q′	Me	F	H	H	F	*s*-butyl	≥200	0.05	0.05	≥4000
5r′	Me	F	H	H	F	*c*-pentyl	>200	0.08	0.08	>2500
5s′	Me	F	H	H	F	*c*-hexyl	>200	0.09	0.07	>2222
9a							150	1.2	1.00	125
9b							86	0.6	0.5	140
10a							147	1.7	1.6	86
10b							>200	0.6	0.5	>333
nevirapine							>200	0.25	0.3	>800
MKC-442							200	0.03	0.04	6666

[a] Data represent mean values of at least two separate experiments. [b] Compound dose required to reduce the viability of mock-infected cells by 50%, as determined by the MTT method. [c] Compound dose required to achieve 50% protection of MT-4 cells from HIV-1-induced cytopathogenicity,as determined by the MTT method. [d] Compound dose required to inhibit the HIV-1 rRT activity by 50%. [e] Selectivity index, CC_{50}/EC_{50} ratio. [f] Higher concentrations could not be achieved because of crystallization of compounds in the culture medium. [g] Not determined.

Analogues bearing a single electron-attracting group (F, Cl, or NO_2) at the 2-, 3-, or 4-position were also suggested for the synthesis in order to enrich the amount of information achievable from SAR data. The above structures were predicted by molecular modeling analyses to attain low-energy conformations fitting into the NNBS cavity with sufficient shape complementarity.

Cytotoxicity, Antiviral Activity, and SAR Studies. On the basis of the above considerations, we synthesized the uracil and thymine derivatives **5a**−**s′** listed in Table 3. Compounds **5a**−**q** are characterized by chlorine, fluorine, or nitro substituents at either the *ortho*, *meta*, or *para* positions of the phenyl ring, and all possess a *sec*-butyl side chain at position 2 of the pyrimidine. Compounds **5r**−**s′** are 2,6-dichloro and 2,6-difluoro derivatives and have different alkylthio side chains.

Title compounds were evaluated for cytotoxicity and anti-HIV-1 activity in MT-4 cells (Table 3) in comparison with MKC-442[32] and nevirapine,[33,34] used as reference drugs. The majority of derivatives are noncytotoxic for MT-4 cells at doses as high as 200 μM, whereas the remaining nine compounds show CC_{50} values ranging from 105 to 182 μM.

Several *ortho*- and *meta*-monosubstituted DABOs (**5d**,**g**,**h**,**j**,**p**) are up to 3 times more active than their parent compounds **9a**,**b**, whereas other monosubstituted derivatives are equally active (**5a**,**e**,**m**) or slightly less

active (**5b**,**k**,**n**). As a rule, the shift of substituents from the *ortho* to the *meta* or *para* position is accompanied by loss of activity. The difference in potency between *ortho*- and *para*-substituted derivatives ranges between 5-fold (**5c** vs **5a**) and 33-fold (**5f** vs **5d**) and is likely due to the slightly unfavorable steric interaction between the 4-substituent and the Trp229 side chain of the NNBS.

In the dihalo-substituted series (compounds **5r**−**s′**), difluoro derivatives are usually more active than the dichloro counterparts. The sole exception is represented by **5j′** which, together with its **5c′**,**q′** *sec*-butyl difluoro homologues, is active at nanomolar concentrations and shows a potency significantly higher than that of nevirapine and comparable to that of MKC-442. Interestingly, also in dihalo-substituted DABOs the alkylthio substituents modulate the anti-HIV-1 potency. However, a peculiar feature of the latter, and in particular of thymine derivatives, is the very small differences in potency among compounds carrying different alkyl substituents in the alkylthio chain.

The above results appear to confirm our hypothesis about the favorable effect of 2,6-dihalogenation related to an attractive π-stacking interaction taking place between the benzene rings of Tyr188 and DABOs. Also consistent with the hypothesis is the fact that the presence of a single electron-withdrawing group at the *ortho* or *meta* position of the phenyl ring of DABOs reduces the beneficial electronic effect on the antiviral activity produced by 2,6-dihalogenation.

Since previous DABO derivatives targeted the HIV-1 RT, the title compounds were also tested in enzyme assays against highly purified recombinant HIV-1 RT using homopolymeric template primers, and their inhibitory activity was expressed as IC_{50}. An excellent correlation was found between the EC_{50} and IC_{50} values indicating that the in vitro antiproliferative activity does entirely reflect the capability of the tested compounds to inhibit the enzyme. This conclusion is strengthened by the fact that, besides being specific inhibitors of the HIV-1 acute infection, DABOs inhibit neither the multiplication of HIV-2 nor that of HIV-1 in chronically infected $H9/III_B$ cells (results not shown).

In conclusion, the new dihalogen-substituted DABOs emerge as noncytotoxic, anti-HIV-1 agents whose potency is comparable to that of MKC-442, the most important of the structurally related HEPT class of NNRTIs.

Experimental Section

Chemistry. Melting points were determined on a Büchi 530 melting point apparatus and are uncorrected. Infrared (IR) spectra (KBr) were recorded on a Perkin-Elmer 297 instrument. ^{1}H NMR spectra were recorded at 200 MHz on a Bruker AC 200 spectrometer; chemical shifts are reported in δ (ppm) units relative to the internal reference tetramethylsilane (Me_4-Si). All compounds were routinely checked by TLC and ^{1}H NMR. TLC was performed on aluminum-backed silica gel plates (Merck DC-Alufolien Kieselgel 60 F_{254}) with spots visualized by UV light. All solvents were reagent grade and, when necessary, were purified and dried by standard methods. Concentration of solutions after reactions and extractions involved the use of a rotary evaporator operating at a reduced pressure of ca. 20 Torr. Organic solutions were dried over anhydrous sodium sulfate. Analytical results are within ±0.40% of the theoretical values. Substituted phenylacetic acids, *N*,*N*-carbonyldiimidazole, iodomethane, 2-iodopropane, 1-iodo-2-methylpropane, 2-iodobutane, 1-iodobutane, cyclopentyl bromide, and cyclohexyl iodide were purchased from Aldrich Chimica, Milan (Italy), and Lancaster Synthesis GmbH, Milan (Italy).

Syntheses. The specific examples presented below illustrate general synthetic methods A−F. As a rule, samples prepared for physical (Tables 1 and 2) and biological (Table 3) studies were dried in high vacuum over P_2O_5 for 20 h at temperatures ranging from 25 to 110 °C, depending on the sample melting point.

Method A. Example: Ethyl 4-(2,6-Dichlorophenyl)-acetylacetate (7p). Triethylamine (8.7 mL, 62.4 mmol) and magnesium chloride (4.64 g, 48.73 mmol) were added to a stirred suspension of potassium ethyl malonate (6.97 g, 40.95 mmol) in dry acetonitrile (50 mL), and stirring was continued at room temperature for 2 h. Then, a solution of the (2,6-dichlorophenylacetyl)imidazolide in dry acetonitrile (50 mL), prepared 15 min before by reaction between 2,6-dichlorophenylacetic acid (4.00 g, 19.49 mmol) and *N*,*N*′-carbonyldiimidazole (3.47 g, 21.40 mmol) in acetonitrile (20 mL), was added. The reaction was allowed to stir overnight at room temperature and then heated at reflux for 2 h. After the mixture had cooled, 13% HCl (50 mL) was cautiously added while keeping the temperature below 25 °C, and the resulting clear mixture was stirred for a further 15 min. The organic layer was separated and evaporated; then the residue was treated with ethyl acetate (50 mL). The aqueous layer was extracted with ethyl acetate (2 × 50 mL), and the organic phases were combined, washed with saturated sodium bicarbonate solution (2 × 100 mL) and brine (100 mL), dried, and concentrated to give pure **7p** (5.3 g): ^{1}H NMR ($CDCl_3$) δ 1.25−1.32 (t, 3H, CH_2CH_3), 3.56 (s, 2H, $COCH_2CO$), 4.17−4.24 (m, 2H, CH_2CH_3), 4.24 (s, 2H, $COCH_2Ar$), 7.16−7.20 (m, 1H, 4-H Ar), 7.30−7.34 (m, 2H, 3,5-H Ar); IR ν 1725, 1700 cm^{-1}. Anal. C, H, Cl.

Method B. Example: 6-(2-Chlorophenylmethyl)-3,4-dihydro-5-methyl-2-thiopyrimidin-4(3*H*)-one (8i). Sodium metal (0.42 g, 0,018 g-atom) was dissolved in 50 mL of absolute ethanol, and thiourea (0.97 g, 12.74 mmol) and ethyl 2-(2-chlorophenylacetyl)propionate (**7i**) (2.34 g, 9.19 mmol) were added to the clear solution. The mixture was heated at reflux for 5 h. After cooling, the solvent was removed, and the residue was dissolved in water (20 mL) and acidified with 2 N HCl. The resulting precipitate was filtered, washed with diethyl ether, and dried in vacuo at 80 °C for 12 h to give **8i** (1.37 g) as a pure solid: ^{1}H NMR (DMSO-d_6) δ 1.63 (s, 3H, C_5-CH_3), 3.90 (s, 2H, CH_2Ar), 7.04−7.09 (m, 1H, 4-H Ar), 7.26−7.30 (m, 2H, 5,6-H Ar), 7.45−7.50 (m, 1H, 3-H Ar), 12.22 (s, 1H, NH exchangeable with D_2O), 12.43 (s, 1H, NH exchangeable with D_2O); IR ν 3200, 2940, 1635 cm^{-1}. Anal. C, H, Cl, N, S.

Method C. Example: 6-(2,6-Difluorophenylmethyl)-3,4-dihydro-5-methyl-2-(methylthio)pyrimidin-4(3*H*)-one (5m′). A mixture of 6-(2,6-difluorophenylmethyl)-3,4-dihydro-5-methyl-2-thiopyrimidin-4(3*H*)-one (**8s**) (0.30 g, 1.12 mmol) and iodomethane (0.32 g, 0.14 mL, 2.24 mmol) in 2 mL of anhydrous DMF was stirred at room temperature for 24 h. The suspension was then diluted with cold water (100 mL) and extracted with ethyl acetate (3 × 50 mL). The combined organic extract was washed with brine (3 × 50 mL), dried, and evaporated to furnish crude **5m′** (0.30 g), which was recrystallized: ^{1}H NMR (DMSO-d_6) δ 2.02 (s, 3H, C_5-CH_3), 2.15 (s, 3H, SCH_3), 3.89 (s, 2H, CH_2Ar), 7.00−7.07 (m, 2H, 3,5-H Ar), 7.26−7.41 (m, 1H, 4-H Ar), 12.53 (broad s, 1H, NH exchangeable with D_2O); IR ν 2950, 1640 cm^{-1}. Anal. C, H, F, N, S.

Method D. Example: 6-(2,6-Difluorophenylmethyl)-3,4-dihydro-2-(1-methylpropylthio)pyrimidin-4(3*H*)-one (5c′). A mixture of 6-(2,6-difluorophenylmethyl)-3,4-dihydro-2-thiopyrimidin-4(3*H*)-one (**8q**) (0.50 g, 2.03 mmol), 2-iodobutane (0.40 g, 0.25 mL, 2.23 mmol), potassium carbonate (0.27 g, 1.95 mmol), and 2 mL of anhydrous DMF was stirred at room temperature for 24 h. After treatment with cold water (200 mL), the solution was extracted with ethyl acetate (3 × 50 mL). The combined organic extract was washed

with brine (3 × 50 mL), dried, and evaporated to furnish crude **5c′**, which was purified by chromatography over silica gel column (eluent: chloroform): ^{1}H NMR ($CDCl_3$) δ 0.89−0.96 (t, 3H, CH_2CH_3), 1.26−1.30 (d, 3H, $CHCH_3$), 1.57−1.67 (m, 2H, CH_2CH_3), 3.74−3.86 (m, 1H, $CHCH_3$), 3.86 (s, 2H, CH_2Ar), 5.95 (s, 1H, C-5 H), 6.82−6.89 (m, 2H, 3,5-H Ar), 7.19−7.24 (m, 1H, 4-H Ar), 13.02 (broad s, 1H, NH exchangeable with D_2O); IR ν 2900, 1640 cm^{-1}. Anal. C, H, F, N, S.

Method E. Example: 2-(Cyclohexylthio)-6-(2,6-dichlorophenylmethyl)-3,4-dihydropyrimidin-4(3*H*)-one (5x). A mixture of 6-(2,6-dichlorophenylmethyl)-3,4-dihydro-2-thiopyrimidin-4(3*H*)-one (**8p**) (0.50 g, 1.74 mmol), cyclohexyl iodide (0.40 g, 0.25 mL, 1.91 mmol), and potassium carbonate (0.24 g, 1.74 mmol) in 2 mL of anhydrous DMF was heated at 80 °C for 15 h. After cooling, the reaction mixture was treated with cold water (100 mL) and extracted with ethyl acetate (3 × 50 mL). The organic layers were collected, washed with brine (3 × 50 mL), dried, and evaporated to furnish crude **5x**, which was purified by chromatography on silica gel column (eluent: *n*-hexane/ethyl acetate/methanol, 12/3/1): ^{1}H NMR ($CDCl_3$) δ 1.26−1.48 (m, 6H, C_3,C_4,C_5 cyclohexane-H), 1.56−1.67 (m, 2H, C_{2eq},C_{6eq} cyclohexane-H), 1.91−1.96 (m, 2H, C_{2ax},C_{6ax} cyclohexane-H), 3.69−3.74 (m, 1H, SCH), 4.17 (s, 2H, CH_2Ar), 5.89 (s, 1H, C_5-H), 7.08−7.16 (m, 1H, 4-H Ar), 7.24−7.32 (m, 2H, 3,5-H Ar), 12.62 (broad s, 1H, NH exchangeable with D_2O); IR ν 2900, 1645 cm^{-1}. Anal. C, H, Cl, N, S.

Method F. Example: 3,4-Dihydro-2-(1-methylpropylthio)-6-(4-nitrophenylmethyl)pyrimidin-4(3*H*)-one (5i). A 65% solution of nitric acid (0.05 mL, 1.09 mmol) was cautiously added to an ice-cooled mixture of 3,4-dihydro-2-(1-methylpropylthio)-6-(phenylmethyl)pyrimidin-4(3*H*)-one (**9a**)[12] (0.30 g, 1.09 mmol) and 98% sulfuric acid (5 mL), and the resulting mixture was stirred at room temperature for 1 h. After treatment with cold water (100 mL), the solution was extracted with ethyl acetate (3 × 50 mL) and the combined organic extract was washed with brine (3 × 50 mL), dried, and evaporated to furnish crude **5i** (0.34 g) that was homogeneous by TLC analysis (SiO_2/*n*-hexane−acetone, 3:1): ^{1}H NMR ($CDCl_3$) δ 0.90−0.97 (t, 3H, CH_2CH_3), 1.29−1.32 (d, 3H, $CHCH_3$), 1.59−1.68 (m, 2H, CH_2CH_3), 3.77−3.87 (m, 1H, $CHCH_3$), 3.87 (s, 2H, CH_2Ar), 6.02 (s, 1H, C_5−H), 7.39−7.43 (d, 2H, 2,6-H Ar), 8.13−8.18 (d, 2H, 3,5-H Ar), 12.82 (broad s, 1H, NH exchangeable with D_2O); IR ν 2950, 1640, 1510, 1335 cm^{-1}. Anal. C, H, N, S.

Molecular Modeling. Molecular modeling studies were performed with the software package SYBYL[27] running on a Silicon Graphics Iris Indigo XS24 workstation. Herein we describe the computational procedure applied to the 2,6-difluoro-DABO (**5r′**); analogues of **5r′** were modeled following a similar approach.

A model of **5r′**, based on the crystal structure of 6-(3-methylphenylmethyl)-2-(2-methylpropylthio)-S-DABO,[35] was created using the SYBYL fragment library. The 2-cyclopentylthio substituent was consistently modeled as a half-chair equatorially substituted conformation.

Conformational energies were calculated with the Tripos force field protocol[26] including the electrostatic contribution. Partial atomic charges were assigned according to the Gasteiger−Hückel method.[36,37] Geometry optimizations were performed with the SYBYL/MAXIMIN2 minimizer by applying the Broyden−Fletcher−Goldfarb−Shanno algorithm[38] and setting a root-mean-square gradient of the forces acting on each atom of 0.05 kcal/mol Å as convergence criterion. Under these conditions, energy minimization reproduced satisfactorily the solid-state geometry of 6-(3-methylphenylmethyl)-2-(2-methylpropylthio)-S-DABO[35] about the thymine and phenylmethyl moieties.

Systematic conformational analyses were carried out using the SYBYL/SEARCH routine to identify low-energy conformations of **5r′**. Torsional angles τ_1−τ_4 (defined in Figure 2) were scanned by 10° increments throughout a 0−350° range. A van der Waals scaling factor of 0.7 was applied to "soften" steric contacts. Such scaling was aimed to minimize the typical limitations of systematic "rigid" search consisting of lack of

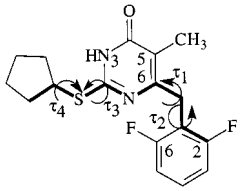

Figure 2.

relaxation for each conformation. The number of output conformations to be examined was reduced by setting the "energy window" (energy difference between the generated conformation and the current minimum) to 2.0 kcal/mol. The resulting conformations were classified in the grid space of torsional angles into a smaller number of "families" using the FAMILY option of the SYBYL/MOLECULAR SPREADSHEET routine. The lowest energy conformer of each family was fully energy-minimized, and among the resulting structures we identified the global minimum energy conformer.

Molecular superimpositions were performed by minimizing the root-mean-square distance between selected pairs of atoms using the SYBYL/FIT and SYBYL/MATCH commands.

The geometry of the nonnucleoside binding site (NNBS) of RT was derived from a 3.0 Å resolution structure of the HIV-1 RT/HEPT complex[14] filed in the Brookhaven Protein Data Bank[28,29] (entry code 1RTI). The NNBS consisted of a set of 69 amino acids located within a distance of 10 Å from any nonhydrogen atom of the bound inhibitor. Hydrogens were added to the unfilled valences of HEPT and of the amino acids according to standard geometries of the Tripos force field. Charges of the NNBS atoms were calculated by the Gasteiger−Hückel method (Lys, Asp, and Glu side chains were modeled in their ionized forms).

Docking of the 2,6-difluoro-DABO (**5r′**) into the NNBS was carried out in two steps. First, the 2-(cyclopentylthio)-5-methyldihydropyrimidinone (CPMP) moiety was superimposed on the thymine ring of HEPT with overlap of the common NHCO fragments. HEPT was removed from the site. Using the SYBYL/DOCK routine, the CPMP moiety was rotated and translated manually within the plane of the pyrimidine ring by monitoring the ligand site interaction energy made up by steric and electrostatic contributions. During this maneuver, the atoms of the 2,6-difluorophenylmethyl substituent of the ligand were ignored by the force field, the hydrogen bond distance between the hydrogen of the pyrimidine 3-NH group and the carbonyl oxygen of Lys101 was monitored, and the torsional angles τ_3 and τ_4 determining the orientation of the 2-cyclopentylthio substituent were adjusted manually. The process, constrained by requirements of (i) coplanarity of the pyrimidine and thymine rings of **5r′** and HEPT and (ii) preservation of the above-mentioned hydrogen bond, ended up until no improvement of the interaction energy was apparently possible.

The docking continued by seeking the optimal position of the previously neglected 2,6-difluorobenzyl group. This was realized using the SYBYL/SEARCH routine. Torsional angles τ_1 and τ_2 were rotated by 10° increments in the 0−350° range. A van der Waals scaling factor of 0.7 was applied to both ligand and site atoms. A limited number of output conformations, very similar to one another, were obtained. A trial active conformation was chosen as that with the lowest volume in common with the protein atoms (this volume was computed using the SYBYL/MVOLUME command).

Geometric optimization of the RT/**5r′** complex was performed to relieve sterically undesirable contacts between ligand and NNBS. The protein backbone atoms were kept fixed. The complex was minimized to an attractive interaction energy of −10 kcal/mol.

The putative active conformation of **5r′**, characterized by an energy of 1.7 kcal/mol above that of the corresponding global minimum conformer, was associated with the following torsional angles: $\tau_1 = -52°$, $\tau_2 = -93°$, $\tau_3 = -27°$, $\tau_4 = -56°$.

Antiviral Assay Procedures. 1. Compounds. Com-

pounds were solubilized in DMSO at 200 mM and then diluted into culture medium.

2. Cells and Viruses. MT-4, C8166, H9/III_B, and CEM cells were grown at 37 °C in a 5% CO_2 atmosphere in RPMI 1640 medium, supplemented with 10% fetal calf serum (FCS), 100 IU/mL penicillin G, and 100 μg/mL streptomycin. Cell cultures were checked periodically for the absence of mycoplasma contamination with a MycoTect Kit (Gibco). Human immunodeficiency viruses type-1 (HIV-1, III_B strain) and type-2 (HIV-2, ROD strain; kindly provided by Dr. L. Montagnier, Paris) were obtained from supernatants of persistently infected H9/III_B and CEM cells, respectively. HIV-1 and HIV-2 stock solutions had titers of 4.5×10^6 and 1.4×10^5 50% cell culture infectious dose ($CCID_{50}$)/mL, respectively.

3. HIV Titration. Titration of HIV was performed in C8166 cells by the standard limiting dilution method (dilution 1:2, four replica wells/dilution) in 96-well plates. The infectious virus titer was determined by light microscope scoring of cytopathicity after 4 days of incubation, and the virus titers were expressed as $CCID_{50}$/mL.

4. Anti-HIV Assays. Activity of the compounds against HIV-1 and HIV-2 multiplication in acutely infected cells was based on the inhibition of virus-induced cytopathicity in MT-4 and C8166 cells, respectively. Briefly, 50 μL of culture medium containing 1×10^4 cells was added to each well of flat-bottom microtiter trays containing 50 μL of culture medium with or without various concentrations of the test compounds. Then 20 μL of an HIV suspension containing 100 (HIV-1) or 1000 (HIV-2) $CCID_{50}$ was added. After a 4-day incubation (5 days for HIV-2) at 37 °C, the number of viable cells was determined by the 3-(4,5-dimethylthiazol-1-yl)-2,5-diphenyltetrazolium bromide (MTT) method.[39] Cytotoxicity of the compounds was evaluated in parallel with their antiviral activity. It was based on the viability of mock-infected cells, as monitored by the MTT method.

5. RT Assays. Assays were performed as previously described.[40] Briefly, purified rRT was assayed for its RNA-dependent polymerase-associated activity in a 50-μL volume containing: 50 mM Tris-HCl (pH 7.8), 80 mM KCl, 6 mM $MgCl_2$, 1 mM DTT, 0.1 mg mL^{-1} BSA, 0.5 OD_{260} unit mL^{-1} template:primer [poly(rC)-oligo$(dG)_{12-18}$], and 10 mM [^{3}H]-dGTP (1 Ci $mmol^{-1}$). After incubation for 30 min at 37 °C, the samples were spotted on glass fiber filters (Whatman GF/A), and the acid-insoluble radioactivity was determined.

Acknowledgment. The authors thank Italian Ministero della Sanità − Istituto Superiore di Sanità − IX Progetto AIDS 1996 (Grants 40A.0.06 and 9403-59) for financial aid. Thanks are also due to Italian MURST (40% funds) and Regione Autonoma Sardegna (Assessorato Sanità) for partial support.

References

(1) Artico, M. Nonnucleoside anti-HIV-1 reverse transcriptase inhibitors (NNRTIs): a chemical survey from lead compounds to selected drugs for clinical trials. *Farmaco* **1996**, *51*, 305−331.
(2) De Clercq, E. Toward Improved Anti-HIV Chemotherapy: Therapeutic Strategies for Intervention with HIV Infections. *J. Med. Chem.* **1995**, *38*, 2491−2517.
(3) De Clercq, E. Antiviral Therapy for Human Immunodeficiency Virus Infections. *Clin. Microbiol. Rev.* **1995**, *8*, 200−239.
(4) Vanhove, G. F.; Gries, J.-M.; Verotta, D.; Sheiner, L. B.; Coombs, R.; Collier, A. C.; Blaschke, T. F. Exposure-Response Relationships for Saquinavir, Zidovudine, and Zalcitabine in Combination Therapy. *Antimicrob. Agents Chemother.* **1997**, *41*, 2433−2438.
(5) De Clercq, E.; Balzarini, J. Knocking out Human Immunodeficiency Virus Through Nonnucleoside Reverse Transcriptase Inhibitors used as single agents or in Combinations: a Paradigm for the cure of AIDS? *Farmaco* **1995**, *50*, 735−747.
(6) Tanaka, H.; Baba, M.; Hayakawa, H.; Sakamaki, T.; Miyasaka, T.; Ubasawa, M.; Takashima, H.; Sekiya, K.; Nitta, I.; Shigeta, S.; Walker, R. T.; Balzarini, J.; De Clercq, E. A New Class of HIV-1-Specific 6-Substituted Acyclouridine Derivatives: Synthesis and Anti-HIV-1 Activity of 5- or 6-Substituted Analogues of 1-[(2-Hydroxyethoxy)methyl]-6-(phenylthio)thymine (HEPT). *J. Med. Chem.* **1991**, *34*, 349−357.
(7) Baba, M.; Shigeta, S.; Tanaka, H.; Miyasaka, T.; Ubasawa, M.; Umezu, K.; Walker, R. T.; Pauwels, R.; De Clercq, E. Highly Potent and Selective Inhibition of HIV-1 Replication by 6-Phenylthiouracil Derivatives. *Antiviral Res.* **1992**, *17*, 245−264.
(8) Botta, M.; Artico, M.; Massa, S.; Gambacorta, A.; Marongiu, M. E.; Pani, A.; La Colla, P. Synthesis, Antimicrobial and Antiviral Activities of Isotrimethoprim and some related Derivatives. *Eur. J. Med. Chem.* **1992**, *27*, 251−257.
(9) Artico, M.; Massa, S.; Mai, A.; Marongiu, M. E.; Piras, G.; Tramontano, E.; La Colla, P. 3,4-Dihydro-2-alkoxy-6-benzyl-4-oxopyrimidines (DABOs): a New Class of Specific Inhibitors of Human Immunodeficiency Virus Type 1. *Antiviral Chem. Chemother.* **1993**, *4*, 361−368.
(10) Tramontano, E.; Marongiu, M. E.; De Montis, A.; Loi, A. G.; Artico, M.; Massa, S.; Mai, A.; La Colla, P. Characterization of the Anti-HIV-1 Activity of 3,4-Dihydro-2-alkoxy-6-benzyl-4-oxopyrimidines (DABOs), New Non-Nucleoside Reverse Transcriptase Inhibitors. *Microbiologica* **1994**, *17*, 269−279.
(11) Massa, S.; Mai, A.; Artico, M.; Sbardella, G.; Tramontano, E.; Loi, A. G.; Scano, P.; La Colla, P. Synthesis and antiviral activity of new 3,4-dihydro-2-alkoxy-6-benzyl-4-oxopyrimidines (DABOs), specific inhibitors of human immunodeficiency virus Type-1. *Antiviral Chem. Chemother.* **1995**, *6*, 1−8.
(12) Mai, A.; Artico, M.; Sbardella, G.; Massa, S.; Loi, A. G.; Tramontano, E.; Scano, P.; La Colla, P. Synthesis and anti-HIV-1 Activity of Thio Analogues of Dihydroalkoxybenzyloxopyrimidines. *J. Med. Chem.* **1995**, *38*, 3258−3263.
(13) Mai, A.; Artico, M.; Sbardella, G.; Quartarone, S.; Massa, S.; Loi, A. G.; De Montis, A.; Scintu, F.; Putzolu, M.; La Colla, P. Dihydro(alkylthio)(naphthylmethyl)oxopyrimidines: Novel Non-Nucleoside Reverse Trasncriptase Inhibitors of the *S*-DABO Series. *J. Med. Chem.* **1997**, *40*, 1447−1454.
(14) Ren, J.; Esnouf, R.; Garman, E.; Somers, D.; Ross, C.; Kirby, I.; Keeling, J.; Darby, G.; Jones, Y.; Stuart, D.; Stammers, D. High-Resolution Structures of HIV-1 RT from four RT-Inhibitor Complexes. *Nature Struct. Biol.* **1995**, *2*, 293−302.
(15) Aroyan, A. A.; Kramer, M. S. Pyrimidine derivatives. Substituted 6-(4′-alkoxybenzyl)pyrimidines. *Arm. Khim. Zh.* **1971**, *24*, 161−166; *Chem. Abstr.* **1971**, *75*, 49022w.
(16) Riegel, B.; Lilienfeld, W. M. The Synthesis of β-Keto Esters by the Decomposition of Acylated Malonic Esters. *J. Am. Chem. Soc.* **1945**, *67*, 1273−1275.
(17) Monostory, J. New derivatives on carbon atom 6 of thiouracil with antithyroidal effects. *An. Asoc. Quim. Argent.* **1952**, *40*, 99−108.
(18) Katagiri, N.; Kato, T.; Nakano, J. Studies on Ketene and Its Derivatives. CIX. Synthesis of Naturally Occurring Anthracene-9,10-diones. *Chem. Pharm. Bull.* **1982**, *30*, 2440−2446.
(19) Miller, W. H.; Dessert, A. M.; Anderson, G. W. The Synthesis of Some 6-Substituted-2-thiouracils. *J. Am. Chem. Soc.* **1948**, *70*, 500−502.
(20) Moody, C. J.; Rahimtoola, K. F. Diels−Alder Reactivity of Pyrano[4,3-b]indol-3-ones, Indole 2,3-Quinodimethane Analogues. *J. Chem. Soc., Perkin Trans. 1* **1990**, 673−679.
(21) Ohkubo, M.; Kuno, A.; Sakai, H.; Sugiyama, Y.; Takasugi, H. Studies on Cerebral Protective Agents. VI. Synthesis of Novel 4-(4-Nitrobenzoyl)pyrimidine and Related Compounds with Anti-anoxic Activity. *Chem. Pharm. Bull.* **1994**, *42*, 1279−1285.
(22) Capozzi, G.; Roelens, S.; Talami, S. A Protocol for the Efficient Synthesis of Enantiopure β-Substituted β-Lactones. *J. Org. Chem.* **1993**, *58*, 7932−7936.
(23) Danel, K.; Nielsen, C.; Pedersen, E. B. Anti-HIV Active Naphthyl Analogues of HEPT and DABO. *Acta Chem. Scand.* **1997**, *51*, 426−430.
(24) Moinet, G.; Dostert, P.; Bourgery, G. Heterocyclic aminoalkoyl derivatives and their therapeutic use. Belg. BE 891,526, June 18, 1982, FR Appl. 80/27,252, Dec 22, 1980; *Chem. Abstr.* **1982**, *97*, 216027q.
(25) Fenner, H.; Teichmann, R. Pyrimido[5,4-b]chinoline−10-Deaza-alloxazine. *Arch. Pharm. (Weinheim)* **1978**, *311*, 115−125.
(26) Clark, M.; Cramer, R. D., III; Van Opdenbosch, N. Validation of the General Purpose Tripos 5.2 Force Field. *J. Comput. Chem.* **1989**, *10*, 982−1012.
(27) SYBYL Molecular Modeling System (version 6.2), TRIPOS Assoc., St. Louis, MO.
(28) Protein Data Bank entry codes 1RTI, 1VRT, 1RTH, 1HNI, 1VRU, 1HNV, 1REV, 1RT1, 1RT2.
(29) Bernstein, F. C.; Koetzle, T. F.; Williams, G. J. B.; Meyer, E. F., Jr.; Brice, M. D.; Rodgers, J. R.; Kennard, O.; Shimanouchi, T.; Tasumi, T. The Protein Data Bank: A Computer Based Archival File for Macromolecular Structures. *J. Mol. Biol.* **1977**, *112*, 535−542.
(30) Schäfer, W.; Friebe, W.-G. F.; Leinert, H.; Mertens, A.; Poll, T.; von der Saal, W.; Zilch, H.; Nuber, B.; Ziegler, M. L. Nonnucleosides Inhibitors of HIV-1 Reverse Transcriptase: Molecular Modeling and X-ray Structure Investigations. *J. Med. Chem.* **1993**, *36*, 726−732.

(31) Hopkins, A. L.; Ren, J.; Esnouf, R. M.; Willcox, B. E.; Jones, E. Y.; Ross, C.; Miyasaka, T.; Walker, R. T.; Tanaka, H.; Stammers, D. K.; Stuart, D. I. Complexes of HIV-1 Reverse Transcriptase with Inhibitors of the HEPT Series Reveal Conformational Changes Relevant to the Design of Potent Non-Nucleoside Inhibitors. *J. Med. Chem.* **1996**, *39*, 1589−1600.

(32) Baba, M.; Shigeta, S.; Yuasa, S.; Takashima, H.; Sekiya, K.; Ubasawa, M.; Tanaka, H.; Miyasaka, T.; Walker, R. T.; De Clercq, E. Preclinical Evaluation of MKC-442, a Highly Potent and Specific Inhibitor of Human Immunodeficiency Virus Type 1 in Vitro. *Antimicrob. Agents Chemother.* **1994**, *38*, 688−692.

(33) Merluzzi, V. J.; Hargrave, K. D.; Labadia, M.; Grozinger, K.; Skoog, M.; Wu, J. C.; Shih, C.-K.; Eckner, K.; Hattox, S.; Adams, J.; Rosenthal, A. S.; Faanes, R.; Eckner, R. J.; Koup, R. A.; Sullivan, J. L. Inhibition of HIV-1 Replication by a Nonnucleoside Reverse Transcriptase Inhibitor. *Science* **1990**, *250*, 1411−1413.

(34) Hargrave, K. D.; Proudfoot, J. R.; Grozinger, K. G.; Cullen, E.; Kapadia, S. R.; Patel, U. R.; Fuchs, V. U.; Mauldin, S. C.; Vitous, J.; Behnke, M. L.; Kluinder, J. M.; Pal, K.; Skiles, J. V.; McNeil, D. W.; Rose, J. M.; Chow, G. C.; Skoog, M. T.; Wu, J. C.; Schmidt, G.; Engel, W. W.; Eberlein, W. G.; Saboe, T. D.; Campbell, S. J.; Rosenthal, A. S.; Adams, J. Novel Nonnucleoside Inhibitors of HIV-1 Reverse Transcriptase. 1. Tricyclic Pyridobenzo- and Dipyridodiazepinones. *J. Med. Chem.* **1994**, *34*, 2231−2241.

(35) Ettorre, A.; Mai, A.; Artico, M.; Massa, S.; De Montis, A.; La Colla, P. 6-(3-Methylbenzyl)-2-(2-methylpropyl)thio-4(3H)-pyrimidinone (DABO 622). *Acta Crystallogr.* **1996**, *C52*, 2115−2117.

(36) Gasteiger, J.; Marsili, M. Iterative Partial Equalization of Orbital Electronegativity. *Tetrahedron* **1980**, *36*, 3219−3228.

(37) Purcel, V. P.; Singer, J. A. A Brief Review and Table of Semiepirical Parameters Used in the Hückel Molecular Orbital Methodology. *J. Chem. Eng. Data* **1967**, *12*, 235−246.

(38) Head, J.; Zerner, M. C. A Broyden-Fletcher-Goldfarb-Shanno Optimization Procedure for Molecular Geometries. *Chem. Phys. Lett.* **1985**, *122*, 264−274.

(39) Pauwels, R.; Balzarini, J.; Baba, M.; Snoeck, R.; Schols, D.; Herdewijn, P.; Desmyster, J.; De Clercq, E. Rapid and Automated Tetrazolium-Based Assay for the Detection of anti-HIV Compounds. *J. Virol. Methods* **1988**, *20*, 309−321.

(40) Tramontano, E.; Cheng, Y.-C. HIV-1 Reverse Transcriptase Inhibition by a Dipyridodiazepinone Derivative: BI-RG-587. *Biochem. Pharmacol.* **1992**, *43*, 1371−1376.

JM980260F